Low-Frequency Raman Spectra of Lysozyme Crystals and Oriented DNA Films: Dynamics of Crystal Water

Hisako Urabe,* Yoko Sugawara,# Mitsuo Ataka,§ and Allan Rupprecht¶

*Tokyo Kasei Gakuin University, Aihara, Machida, Tokyo 194-02, Japan; #School of Science, Kitasato University, Kitasato, Sagamihara, Kanagawa 228, Japan; §National Institute of Bioscience and Human Technology, Higashi, Tsukuba, Ibaraki 305, Japan; and ¶Division of Physical Chemistry, Arrhenius Laboratory, University of Stockholm, S-106 91 Stockholm, Sweden

ABSTRACT We observed low-frequency Raman spectra of tetragonal lysozyme crystals and DNA films, with varying water content of the samples. The spectra are fitted well by sums of relaxation modes and damped harmonic oscillators in the region from ~1 cm^{-1} to 250 cm^{-1}. The relaxation modes are due to crystal water, and the distribution of relaxation times is determined. In wet samples, the relaxation time of a small part of the water molecules is a little longer than that of bulk water. The relaxation time of a considerable part of the crystal water, which belongs mainly to the secondary hydration shell, is an order of magnitude longer than that of bulk water. Furthermore, the relaxation time of some water molecules in the primary hydration shell of semidry samples is shorter than we expected. Thus we have shown that low-frequency Raman measurements combined with properly oriented samples can give specific information on the dynamics of hydration water in the ps range. On the other hand, we concluded, based on polarized Raman spectra of lysozyme crystals, that the damped oscillators correspond to essentially intramolecular vibrational modes.

INTRODUCTION

Water molecules play an important role in the function of proteins, nucleic acids, and other biological macromolecules, by maintaining their tertiary structure. The structure of the hydration shell of biomolecules in an aqueous solution is considered to be similar to that of ions. There are two kinds of hydration shell: the primary hydration shell and the secondary hydration shell (Eisenberg and Kauzmann, 1969; Kuntz and Kauzmann, 1974). The water molecules in the primary hydration shell are bound directly to solute molecules, and are further classified into internal water and peripheral water for protein molecules. The water molecules in the secondary hydration shell have a character intermediate between those of the primary hydration shell and bulk water. The relaxation time of water molecules in these hydration shells has been determined by NMR and dielectric relaxation measurements. The observed nature of relaxation is slightly different, depending on the methods. The order of relaxation time of water in the primary hydration shell was reported to be 10^{-6} s (Kuntz and Kauzmann, 1974). Recently it was suggested that there are water molecules with shorter relaxation times τ of 10^{-10} s in the primary hydration shell (Pethig, 1992, and references therein; Otting and Wunthrich, 1989; Brunne et al., 1993). On the other hand, the dielectric relaxation time of bulk water at room temperature is 0.8×10^{-11} s (20 GHz) (Eisenberg and Kauzmann, 1969), and the relaxation time determined by low-frequency Raman scattering is 0.7×10^{-12} s (Mizoguchi et al., 1992). This difference suggests that Raman measurements detect a kind of relaxation that is different from dielectric relaxation.

The structure of biological macromolecules in an aqueous solution is considered to be essentially similar to that in a crystalline state, because sufficient water molecules are contained in a crystal. Crystal water is also classified into groups that correspond to the hydration shells in an aqueous solution. The location of some water molecules is determined by x-ray crystallographic analysis. These water molecules correspond mainly to those in the primary hydration shell and partly to those in the secondary hydration shell. It should be noted, however, that not all of the water molecules in the primary hydration shell are determined by x-ray analysis. Recently, low-temperature x-ray studies on protein crystals have given a more precise picture of hydration shells (Young et al., 1993; Kurinov and Harrison, 1995). On the other hand, low-temperature calorimetry of biomolecules is a powerful tool for estimating the number of nonfreezing water molecules. Nonfreezing water is regarded to be the same as the bound water in the primary hydration shell (Kuntz and Kauzmann, 1974).

The estimation of the relaxation time of hydration water by Raman spectroscopy was already done in the course of freezing of DNA gel (Tominaga et al., 1985). Under the assumption of a coupling between a relaxation mode of water molecules and the lowest-frequency oscillation mode of DNA, they obtained the relaxation time by fitting the low-frequency region. The relaxation times of the primary and secondary hydration water in DNA films were also obtained from the Brillouin shift as 10^{-11} s and 10^{-12} s, respectively (Tao et al., 1987). Weidlich fitted the low-frequency Raman spectra of calf thymus DNA films at various relative humidity conditions by sums of several damped harmonic oscillators (Weidlich, 1989; Weidlich et

Received for publication 10 March 1997 and in final form 14 November 1997.

Address reprint requests to Dr. Hisako Urabe, Tokyo Kasei Gakuin University, 2600 Aihara, Machida, Tokyo 194-0292, Japan. Tel.: 81-427-82-1997; Fax: 81-427-82-9880: E-mail: l00419@simail.ne.jp.

0006-3495/98/03/1533/08 $2.00

al., 1990). He ignored the central component, the shape of which strongly depends on the water content of the film.

Here we used lysozyme crystals and DNA films to clarify the low-frequency dynamics of hydration water and macromolecules by Raman spectroscopy. Making use of large-size transparent lysozyme crystals and well-ordered DNA films, in addition to the improvement of spectrometers, we successfully obtained nontrivial Raman spectra in the range from ~ 1 cm^{-1} at room temperature.

We tried to determine the relaxation time of water molecules in these samples by fitting low-frequency Raman spectra from 1 cm^{-1} to 250 cm^{-1} to a simple sum model of relaxation modes and damped harmonic oscillation modes. The relaxation time was obtained on the samples with different water content. We expect to obtain mainly the dynamical feature of hydration water with a relaxation time of 10^{-12} to 10^{-11} s.

As for the noncentral component, the low-frequency Raman spectra of proteins contain broad bands in 10–200 cm^{-1} (Brown et al., 1972; Genzel et al., 1976). The spectral shape depends on the protein state (e.g., solution, crystalline, denatured, or dried). The origin of the low-frequency response is not yet clear, although some calculations have been carried out (Colaianni and Nielsen, 1995). Lysozyme is a typical globular protein, which is easily crystallized in a tetragonal form a with space group of $P4_32_12$ (Steinrauf, 1959). This crystal symmetry is convenient for analyzing the polarized Raman spectra. We obtained polarized spectra in various scattering geometries. We estimate the role of intermolecular interaction on the low-frequency Raman spectra, by comparing the spectra with different phonon propagation directions.

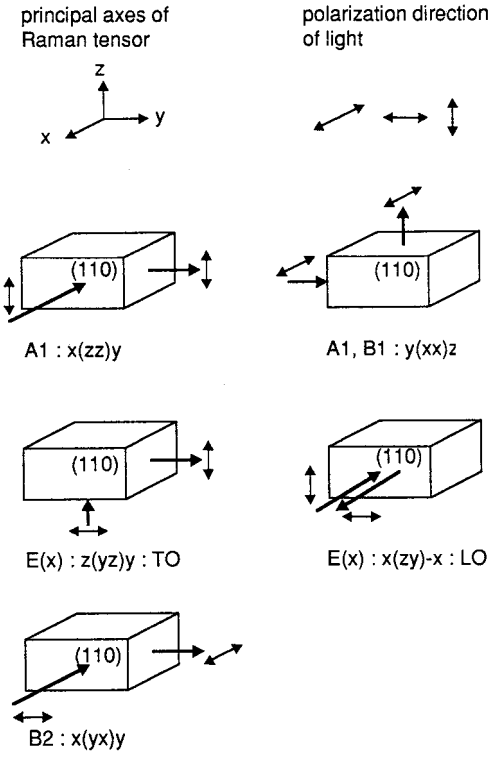

FIGURE 1 Raman scattering geometries for each Raman tensor component. ← or → represents the direction of incident and scattered light. ↔ represents the polarization direction of light. A1: $x(zz)y$ denotes that the scattering geometry with the z polarized incident light from the x direction and the z polarized scattered light in the y direction belongs to the Raman tensor component α_{zz}, which corresponds to the A1 symmetry vibration.

EXPERIMENT AND ANALYSIS

Lysozyme crystals were grown in a solution with a $NiCl_2$ density gradient (Ataka, manuscript in preparation). The crystal data determined by precession photographs are crystal form tetragonal, $a = 79.0(9)$ and $c = 37.2(2)$ Å. They coincide with those of lysozyme crystals grown from a NaCl solution (Steinrauf, 1959) within experimental errors. The growing faces, (1 1 0), (1 −1 0), and (1 0 1), are the same as those of NaCl-lysozyme crystals.

The crystal size used for Raman measurements was about $2 \times 2 \times 2$ mm^3. Three types of lysozyme crystals were used; one is as grown crystal whose water content is estimated to be ~34 w/w % (Steinrauf, 1959) (a wet crystal); the second is a slowly semidried crystal at 50% r.h. (a semidry crystal); the last is a dried crystal equilibrated at ~30% r.h. (a dry crystal). To estimate the water content of dry crystals, we measured the weight increase of crystals at 95% r. h. for several days. The water content of dry crystals was determined to be 8–9 w/w %, that is, ~1/5 of wet crystals. This coincides with the value reported by Morozov et al. (1988).

The scattering geometries adopted in this study are shown in Fig. 1 together with the corresponding Raman tensor components of point group 422 crystals, which corresponds to the space group $P4_32_12$. We examined several different scattering geometries for each Raman tensor component, to obtain the dependence of the Raman spectra on the phonon propagation directions.

A film of oriented salmon testes NaDNA (Fluka) with a thickness of 0.1 mm was prepared with a wet spinning method (Rupprecht, 1966). It contained ~1% NaCl by dry weight (Rupprecht and Forslind, 1970). The film was kept in a closed cell with a saturated salt solution to maintain desired relative humidities. We obtained depolarized spectra with right angle scattering geometry.

Raman spectra at room temperature were obtained with a double grating spectrometer of Jobin-Yvon U-1000, with photon counting electronics. The spectral resolution was <0.5 cm^{-1} for the <10-cm^{-1} region and ~2 cm^{-1} for the 10–250-cm^{-1} region. The excitation was made by a 488-nm line of an Ar ion laser, with laser power less than 10 mW at a sample point. We confirmed, by changing the slit width, that the central component is not due to elastic scattering.

Raman spectra are analyzed in the following way. Raman intensity is represented as

$$I(\omega) = B(\omega)\chi''(\omega) \tag{1}$$

$$B(\omega) = n(\omega) + 1, \quad n(\omega) = \{\exp(h\omega/kT) - 1\}^{-1} \tag{2}$$

$$I_s(\omega) = \chi''(\omega)/\omega \tag{3}$$

where $I(\omega)$ and $\chi''(\omega)$ are observed Raman intensity and the imaginary part of dynamic susceptibility, respectively. $B(\omega)$ is the temperature factor. The symmetrized intensity $I_s(\omega)$ is defined in Eq. 3. The Raman spectra of lysozyme crystals and DNA films are assumed to be represented by sums of several damped harmonic oscillation modes (DHO) and relaxation modes. Then $\chi''(\omega)$ is written as follows:

$$\chi''(\omega) = \sum_i \frac{D_i\omega_{0i}^2\gamma_i\omega}{(\omega_{0i}^2 - \omega^2)^2 + \omega^2\gamma_i^2} + \sum_i \frac{R_i\omega\tau_i}{1 + \omega^2\tau_i^2} \tag{4}$$

D_i, ω_{0i}, and γ_i are the oscillation strength, frequency, and damping constant of the ith damped harmonic oscillator, respectively. R_i and τ_i are the intensity and relaxation time of the ith relaxation mode, respectively.

We carried out a least mean-squares fit on both $\chi''(\omega)$ and $I_s(\omega)$, to obtain the best-fit parameters that represent well both the central and noncentral regions.

RESULTS

Some examples of the Raman spectra of a wet lysozyme crystal in various scattering geometries are shown in Fig. 2. The principal axes of the Raman tensor of the crystal, which are represented by x, y, and z, are parallel to [1 1 0], [1 −1 0], and [0 0 1]. This situation is convenient for separating each Raman tensor component. We measured two scattering geometries, $x(zz)y$ and $y(xx)z$, for the A1 and B1 symmetry modes; three scattering geometries, $x(yx)z$, $z(yx)y$, and $x(yx)y$, for the B2 mode; and five geometries, $x(zy)z$, $x(zx)z$, $x(zy)$-x, $y(xz)x$ and $z(yz)y$, for the $E(x)$ or $E(y)$ modes. $E(x)$ or $E(y)$ modes are polar, so that we can distinguish between transverse optical (TO) and longitudinal optical (LO) phonon modes. The $x(zx)z$ geometry corresponds to the $E(y)$ phonon mode propagating in the xz plane, i.e., this is a TO phonon. The $x(zy)$-x geometry corresponds to the LO phonon propagating along the x direction. The spectra did not depend on phonon propagation directions. The spectra of $z(yz)y$, $x(zy)$-x and $x(zy)z$, which all belong to the $E(x)$ symmetry, are found to be the same. For B2 modes, the spectra show no difference between the two scattering geometries, $z(yx)y$ and $x(yx)y$. The difference among the Raman spectra in various scattering geometries is concluded to be due to the Raman tensor symmetry, i.e., Raman spectra depend only on the Raman tensor components.

In Fig. 3, the spectra of a semidry lysozyme crystal are shown for the same scattering geometries as those in Fig. 2. It can be noticed that the differences among these spectra are smaller than those of a wet crystal.

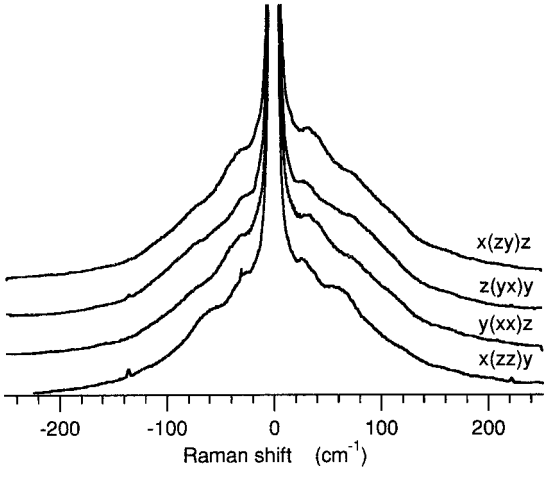

FIGURE 2 Raman spectra of wet lysozyme crystals in various scattering geometries.

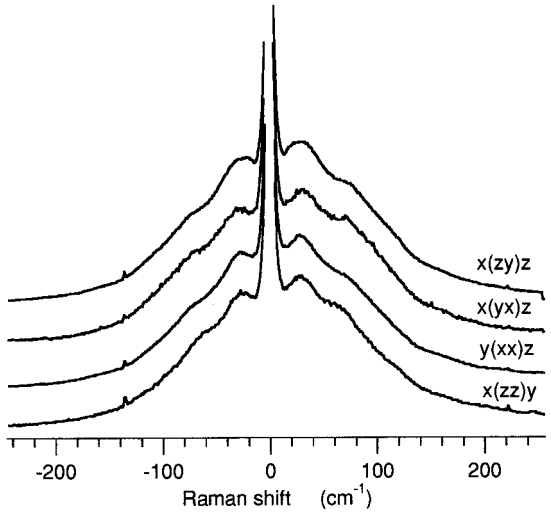

FIGURE 3 Raman spectra of semidry lysozyme crystals in various scattering geometries.

The spectrum of a dry lysozyme crystal is shown in Fig. 4, together with the spectra of wet and semidry crystals in the same scattering geometry. Note that the intensity of the central component decreases with decreasing water content. There is no difference among spectra of dry crystals in different scattering geometries. This result suggests that dry crystals lose crystallinity and become isotropic.

The Raman spectra of a wet lysozyme crystal are fitted by sums of five damped harmonic oscillators (DHOs) and two relaxation modes. The fitting parameters for $x(zy)z$ geometry are listed in the left column of Table 1. The fitting parameters have some minor errors due to the baseline correction of each Raman spectrum. The frequencies and damping constants of DHOs depend on the Raman tensor symmetry. However, the relaxation times of relaxation modes are independent of scattering geometries.

We cannot fit the spectra of semidry and dry lysozyme crystals by sums of DHOs and relaxation modes. The fitting is carried out, excluding the region below 10 cm^{-1}, i.e., the

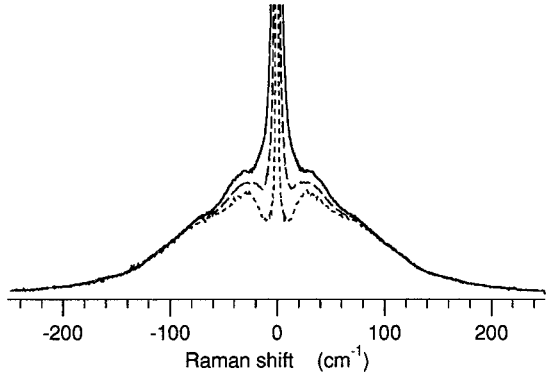

FIGURE 4 Raman spectra $I_s(\omega)$ of wet, semidry, and dry lysozyme crystals in the $x(zy)z$ geometry. The solid line, dashed line, and dotted line correspond to wet, semidry, and dry crystals, respectively.

TABLE 1 Fitting parameters for wet, semidry, and dry lysozyme crystals with scattering geometries of *x(zy)z*

	Wet		Semidry		Dry	
R_1, τ_1 (s)*	20	1×10^{-11}		—		—
R_2, τ_2 (s)	0.6	1.3×10^{-12}		—		—
D_1, $\omega_{01} \pm \gamma_1$#	0.2	17 ± 7	0.5	24 ± 23	1.2	27 ± 16
D_2, $\omega_{02} \pm \gamma_2$	9.8	45 ± 48	7.4	45 ± 50	3.0	42 ± 29
D_3, $\omega_{03} \pm \gamma_3$	10.4	85 ± 66	10.2	86 ± 71	13.1	83 ± 78
D_4, $\omega_{04} \pm \gamma_4$	1.3	112 ± 35	1.3	114 ± 42	3.6	114 ± 65
D_5, $\omega_{05} \pm \gamma_5$	14.2	183 ± 270	5.7	132 ± 161	3.2	167 ± 132

*R_i and τ_i are the intensity and relaxation time of the ith relaxation mode, respectively. Intensities are normalized with the intensity at $\sim$100 cm^{-1}.
#D_i, ω_{0i}, and γ_i are the oscillation strength, frequency, and damping constant of the ith damped harmonic oscillator, respectively.

central components due to relaxation modes are neglected. The fitting parameters of DHOs are shown in Table 1.

The results of the fitting are shown in Fig. 5, *a* and *b*, for wet and semidry crystals, respectively. For a semidry crystal, the residuals between measured spectra and the addition of DHOs are presented instead of relaxation modes.

Raman spectra of A form and B form DNA are shown in Fig. 6, together with the fitted curves. The spectra are fitted by sums of two or three relaxation modes and four or five DHOs. The fitting parameters are listed in Table 2. The fitting parameters for DHOs obtained by Weidlich (1989), who neglected the central component, are also listed in the same table. The spectra of A form and B form DNA are completely fitted by this procedure.

The fitting parameters of relaxation modes with longer relaxation times have ambiguity, because they are beyond the apparatus resolution. However, it can be concluded that there exist relaxation modes whose relaxation times are longer than 1×10^{-11} s (0.5 cm^{-1}). Despite the resolution limit, we note that the relaxation times of a wet lysozyme crystal and a B form DNA film are of equal order.

DISCUSSION

Low-frequency spectra are well fitted by sums of several damped harmonic oscillators (DHOs) and relaxation modes. We carried out the fitting based on three different models, the coupled mode model on B-DNA proposed by Tominaga et al. (1985), a symmetrized form of the coupled mode model, and a simple sum model. We cannot fit the spectra using the equation that appears as Equation 3 in Tominaga

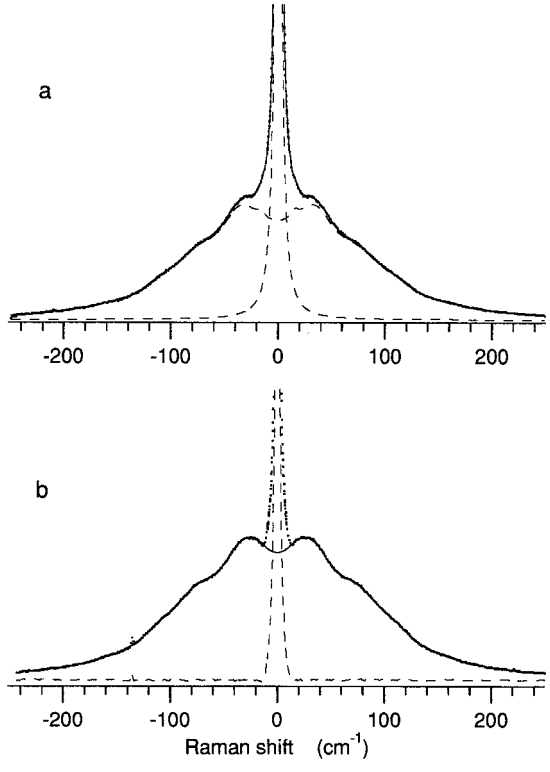

FIGURE 5 Measured and fitted Raman spectra of lysozyme crystals. (*a*) Fitting for a wet crystal. The dots and solid line represent measured and fitted spectra, respectively. Two dashed lines correspond to the addition of relaxation modes and the addition of DHOs. (*b*) Fitting for a semidry crystal. The dots and solid line represent measured and fitted spectra, respectively. The dashed line represents the residual between measured and fitted spectra.

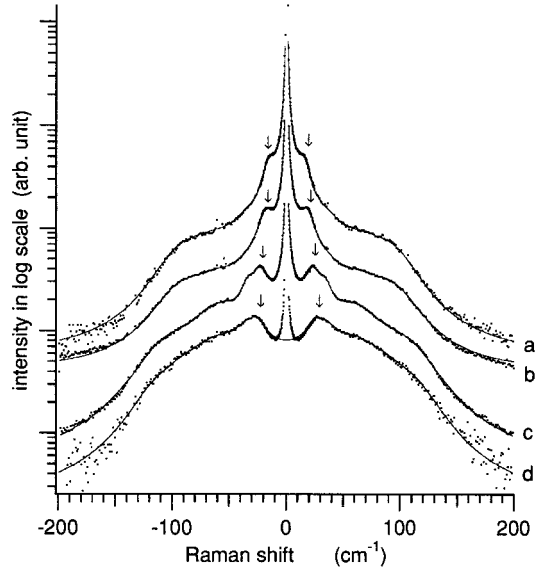

FIGURE 6 Raman spectra I_s (ω) of DNA films with various water contents on a log scale. The dots and solid lines represent measured and fitted spectra, respectively. The S mode is indicated by arrows. (*a*) B form DNA at 100% r. h. (*b*) B form DNA at 95% r. h. (*c*) A form DNA at 75% r. h. (*d*) disordered DNA.

TABLE 2 Fitting parameters for DNA films with various water contents

	B (100% r.h.)		*B* (93% r.h.)		*A* (75% r.h.)		Disorder	
R_1, τ_1 (s)*	9×10^2	5×10^{-11}	6×10	5×10^{-11}	2×10	5×10^{-11}		—
R_2, τ_2 (s)	1.8	0.9×10^{-12}	1.7	1×10^{-12}	0.9	1.6×10^{-12}		—
R_3, τ_3 (s)	0.3	0.7×10^{-12}	0		0			—
D_1, $\omega_{01} \pm \gamma_1$#	3.1	18 ± 15	2.7	21 ± 16	1.6	25 ± 15	0.5	27 ± 14
		(18 ± 18		22 ± 16		26 ± 18		28 ± 19)
D_2, $\omega_{02} \pm \gamma_2$	1.6	40 ± 35	0.8	37 ± 27	0.6	35 ± 13	0.8	37 ± 20
		(39 ± 23		34 ± 17		35 ± 13		39 ± 22)
D_3, $\omega_{03} \pm \gamma_3$	2.3	75 ± 64	2.2	70 ± 60	4.4	70 ± 61	3.3	69 ± 63
		(74 ± 55		70 ± 61		70 ± 57		72 ± 67)
D_4, $\omega_{04} \pm \gamma_4$	1.5	98 ± 51	1.8	99 ± 54	1.1	112 ± 51	1.3	96 ± 58
		(96 ± 37		93 ± 47		95 ± 39		95 ± 47)
D_5, $\omega_{05} \pm \gamma_5$	0		0		0		0.6	118 ± 49
				(112 ± 41		116 ± 36		114 ± 55)

*R_i and τ_i are the intensity and relaxation time of the ith relaxation mode, respectively. Intensities are normalized with the intensity at ~100 cm^{-1}.
#D_i, ω_{0i}, and γ_i are the oscillation strength, frequency, and damping constant of the ith damped harmonic oscillator, respectively. The fitting parameters obtained by Weidlich (1989) are listed in parentheses.

et al. (1985) and is the same as Eq. A2 in Tao et al. (1987). This equation is valid, when the driving force works only on the harmonic oscillator. On the other hand, the spectra can be fitted by the Eq. 5, which is the symmetrized form of the above-mentioned equation.

$$\chi(\omega) = D_1/(\chi_{d1^{-1}}(\omega) - c/\chi_{r1^{-1}}(\omega)) + R_1/(\chi_{r1^{-1}}(\omega) - c/\chi_{d1^{-1}}(\omega)) \quad (5)$$

where $\chi_{d1}(\omega)$ and $\chi_{r1}(\omega)$ are the dynamic susceptibilities of the lowest frequency damped harmonic oscillator and the highest intensity relaxation mode, respectively. In this equation, the paremeter c, the coupling constant, is used as the additional fitting parameter to the simple sum model. We cannot detect the difference between the results of fitting by the symmetrized equation and by the simple sum model. Thus we concluded that the simple sum model is enough to represent the spectra.

We first discuss the central components of lysozyme crystals and DNA films. The intensity of the central component (relaxation modes) reduces drastically with a decrease in water content, as shown in Figs. 4 and 6. This observation suggests that the main part of the central component is due to water molecules, rather than very low-frequency lattice vibrations, or relaxation between different conformations of protein and DNA molecules (jumping between adjacent energy minima). Thus we continue this discussion by assuming that the central component represents the relaxation of crystal water.

Before discussing our results in detail, we briefly summarize the number of water molecules in lysozyme crystals and DNA films. Wet tetragonal lysozyme crystals contain 33.5 w/w% water (Steinrauf, 1959), that is, ~400 mol H_2O/mol lysozyme. The number of water molecules whose positions are determined by x-ray analysis at room temperature is ~100, and that by low-temperature x-ray studies is ~100–200 (Young et al., 1993; Kurinov and Harrison, 1995). The number of nonfreezing waters determined by calorimetric study on solid state lysozyme is ~240–300 mol H_2O/mol lysozyme (Kuntz and Kauzmann, 1974; Mrevlishvili, 1984).

The water content of the dry lysozyme crystals is ~20% of that of wet crystals, i.e., 320 mol H_2O/mol lysozyme are lost by drying. This result indicates that part of the water molecules, which are non-freezing and observed by the x-ray diffraction studies, are lost by drying.

The water loss was also observed by Kachalova et al. (1991) in the case of a hydrated triclinic lysozyme crystal. They reported that a crystal of triclinic form loses 80% of ~230 mol water molecules/mol lysozyme in a wet crystal, keeping crystallinity, when it is dried by silica gel. In contrast, x-ray diffraction work (Kachalova et al., 1991) and polarized Raman scattering (this work) indicate that crystallinity is lost when a tetragonal lysozyme crystal dries. A dry crystal has no lattice periodicity, and the location and/or orientation of lysozyme molecules seem to be disordered.

The water content of typical A form and B form DNA films was reported as ~0.4 gH_2O/g DNA (~15 water molecules/bp) and 1.0 gH_2O/gDNA (~38 water molecules per one base pair), respectively (Falk et al., 1962; Urabe and Tominaga, 1982; Lindsay et al., 1988). In dry DNA the molecules are distorted (Falk et al., 1963) and the crystal structure has collapsed (Lindsay et al., 1988). We will refer to this sample as disordered DNA.

We carried out a differential scanning calorimetry (DSC) measurement on lysozyme crystals and DNA films (manuscript in preparation). When wet lysozyme crystals and B form DNA films are cooled below −50°C, ice is formed. In contrast, semidry and dry lysozyme crystals and A form DNA films show no ice formation. Therefore, the dry samples contain only nonfreezing water.

Now we discuss the results obtained by the fitting of Raman spectra. The central component is fitted by the addition of two Debye-type relaxation modes. The fitting is unsuccessful when a single Debye mode or other modified

Debye type mode (described by Eq. 6) is used.

$$\chi(\omega) = \frac{A}{1 - (i\omega\tau)^{\beta}} \tag{6}$$

The central component cannot be represented by a single typical relaxation time. It needs at least two typical relaxation times which spread over one order.

We continue our discussion on the central component in the order of wet samples to dry samples, referring both to lysozyme and DNA.

The shortest relaxation time obtained is 0.7 ps for B-DNA at ~100% r.h., although the intensity is very weak. The relaxation time is similar to that of bulk water at 25°C (0.7×10^{-12} s) determined by Raman spectroscopy (Mizoguchi et al., 1992). Furthermore, the next shortest relaxation time of the crystal water of wet lysozyme crystals and B-DNA films, 1 ps, is slightly longer than that of bulk water. These results indicate that a small part of the water molecules in wet lysozyme crystals and B-DNA films has a character similar to that of bulk water. The intensities of the relaxation modes mentioned above decrease when the sample is dried.

The longer relaxation time ($\sim 10^{-11}$ s) obtained for wet lysozyme crystals and B-DNA films is less than or equal to the limit of Raman measurements, i.e., the fitted width of the relaxation mode is of the same order as the apparatus resolution of 0.5 cm^{-1} at minimum. Thus we can say only that there exist strong relaxation modes whose relaxation times are longer than 10^{-11} s. The intensities of these modes are much larger than that of the mode with a shorter relaxation time mentioned above. Thus it is possible that these modes correspond to the relaxation of water molecules in the so-called secondary hydration shell. The relaxation time is expected to be distributed in a wide range from that of bulk water to that of bound water, and our experiments reveal that the relaxation time of a considerable portion of water in the secondary hydration shell is of the order of 10^{-11} s.

This relaxation mode appears not only in wet samples, but also in semidry lysozyme crystals and A-DNA films, although the intensity is much smaller in these samples than in the wet samples mentioned above. This immediately suggests that water molecules whose relaxation time is about one order of magnitude longer than that of bulk water even exist in semidry lysozyme crystals or A-DNA films. Furthermore, we obtain the 2-ps relaxation mode with very low intensity for A form DNA. In these samples, freezing water does not exist, i.e., almost all water molecules are in the primary hydration shell. In other words, a small part of nonfreezing water must have the relaxation time of $\sim 10^{-11}$ s.

Otting et al. (Otting and Wunthrich, 1989; Brunne et al., 1993) estimated the lifetime of water in the primary hydration shell by NMR. They obtained $\sim 3 \times 10^{-10}$ s for small protein molecules, bovine pancreatic trypsin inhibitor (BPTI), in an aqueous solution. Dielectric relaxation measurements also indicated the existence of rapid relaxation in solid-state protein samples (Pethig, 1992, and references therein). Our results also strongly suggest that part of the water molecules in the primary hydration shell in solid-state samples have a short relaxation time, comparable to that in liquid samples.

The relaxation times of the primary and secondary hydration waters obtained by Brillouin scattering for DNA films (Tao et al., 1987) and those obtained by Raman scattering for DNA gels (Tominaga et al., 1985) are on the same order as the values obtained here.

We conjecture that the relaxation time of water molecules correlates with their crystallographic temperature factor. In lysozyme crystals, part of the water molecules in the primary hydration shell have rather large temperature factors, and their relaxation time may be short. This consideration is supported by the result that not all of the positions of nonfreezing water molecules are determined by x-ray studies. These water molecules may be lost by further drying. In addition, part of the water molecules in the primary hydration shell with smaller temperature factors can also be lost in the drying process, judging from the large amount of water removed by drying. Here this situation can be compared to the dehydration process of Na_2ATP crystals (Sugawara et al., 1991). The temperature factors of some of the water molecules that are directly bound to an ATP molecule are smaller than those of some of the water molecules hydrated to sodium ions. In the case of Na_2ATP crystals, part of the water molecules with small temperature factors in the primary hydration shell are lost before those with larger temperature factors.

The intensities of the central components in dry lysozyme crystals and disordered DNA films are very weak, but are still observable. We consider this to be due primarily to intermolecular motion and/or to technical ambiguity. In these samples, there exist only water molecules strongly bound to proteins or DNA.

We cannot find a significant difference in relaxation times between lysozyme and DNA samples. From a Raman spectroscopic point of view, the dynamical feature of hydration water of these samples is similar.

Finally, we should note the fact that the relaxation mode appears, even if the network of water molecules is not the same as that of bulk water (Mizoguchi et al., 1992). Therefore, the origin of the relaxation mode is not a relaxation of the network structure, but a more localized relaxation of one or a few water molecules.

We now discuss DHOs. The fitting parameters of DHOs of DNA films show excellent agreement with the values obtained by Weidlich (Weidlich, 1989; Weidlich et al., 1990) (Table 2). Although there may be some ambiguities for such broad bands, the fitting parameters of the lowest frequency mode, which we called the S mode in our previous paper (Urabe et al., 1991), have less uncertainty. The S mode is a well-defined mode whose apparent peak frequency and the fitted frequency depend on the water content of the sample (see also Fig. 6 and Table 2). We cannot say whether other peaks correspond to single vibration modes.

In the case of DHOs of lysozyme crystals, the spectra of wet lysozyme crystals are fitted by sums of five DHOs (D1, D2, D3, D4, and D5), in addition to the two relaxation

modes (R1 and R2). In some cases, the lowest frequency DHO (D1) cannot be fitted because of its low intensity.

When we measure the same Raman tensor component, the spectra and the fitting parameters are the same within experimental errors, even if the scattering geometry is different. In ordinary dielectric crystals, the frequency of TO phonons (ω_{TO}) is smaller than that of LO phonons (ω_{LO}), according to the simplest form LST (Lyddane-Sachs-Teller) relation:

$$\omega_{LO^2}/\omega_{TO^2} = \epsilon_0/\epsilon_\infty > 1 \quad (7)$$

The result that ω_{TO} is the same as ω_{LO} for the E symmetry modes suggests that phonon-like intermolecular interaction does not exist. Therefore, we conclude that there is little long-range electric repulsion among molecules for these modes. Furthermore, the frequencies of pure translational and rotational motions of lysozyme molecules are thought to be much lower than those measured by Raman scattering. Thus the low-frequency modes are essentially intramolecular modes, although some coherence should exist. This is a new finding deduced from our polarized Raman measurements on crystalline samples.

An assembly of macromolecules exhibits many normal modes, and low-frequency Raman spectra are thought to represent the densities of states of these normal modes (Shuker and Gammon, 1970). It is noteworthy that the observed spectra could be regarded as the superposition of four or five well-resolved components, instead of a continuum.

It will be meaningful to compare these spectra with the results of normal mode calculations of a lysozyme molecule. We will discuss the origin of characteristic frequencies in a future publication, together with the comparison of spectra of other protein crystals.

CONCLUSION

We obtained low-frequency Raman spectra of lysozyme crystals and DNA films in the region from 1 cm^{-1} to 250 cm^{-1}, making use of appropriate methods of sample preparation. The spectra are fitted by sums of several damped harmonic oscillators and relaxation modes. The relaxation modes originate from the motion of crystal water, and we determine their relaxation time. In wet samples, the relaxation time of a small part of the water molecules is a little longer than that of bulk water. The relaxation time of a considerable part of crystal water, which belongs mainly to the secondary hydration shell, is an order of magnitude longer than that of bulk water. Furthermore, the relaxation time is $\sim 10^{-11}$ s for some water molecules in semidry samples, which include only nonfreezing water. The DHO modes of lysozyme crystals are assigned essentially to intramolecular vibrations, judging from the dependence on the phonon propagation direction.

This work was supported partly by grants-in-aid from the Ministry of Education, Science, and Culture of Japan to HU and YS, and a grant for Biodesign Research Programs from the Institute of Physical and Chemical Research (RIKEN) to YS. AR acknowledges support from the Swedish Medical Reserch Council.

REFERENCES

Brown, K. G., S. C. Erfurth, E. W. Small, and W. L. Peticolas. 1972. Conformationally dependent low-frequency motions of proteins by laser Raman spectroscopy. *Proc. Natl. Acad. Sci. USA.* 69:1467–1469.

Brunne, R. M., E. Liepinsh, G. Otting, K. K. Wunthrich, and W. F. van Gunsteren. 1993. Hydration of proteins. *J. Mol. Biol.* 231:1040–1048.

Colaianni, S. E. M., and O. F. Nielsen. 1995. Low-frequency Raman spectroscopy. *J. Mol. Struct.* 347:267–283.

Eisenberg, D., and W. Kauzmann. 1969. The Structure and Properties of Water. Oxford University Press, Oxford.

Falk, M., K. A. Hartmann, Jr., and R. C. Lord. 1962. Hydration of deoxyribonucleic acid. I. A gravimetric study. *J. Am. Chem. Soc.* 85: 3843–3846.

Falk, M., K. A. Hartmann, Jr., and R. C. Lord. 1963. Hydration of deoxyribonucleic acid. III. A spectroscopic study of the effect of hydration on the structure of deoxyribonucleic acid. *J. Am. Chem. Soc.* 85:391–394.

Genzel, L., F. Keilmann, T. P. Martin, G. Winterling, and Y. Yacoby. 1976. Low-frequency Raman spectra of lysozyme. *Biopolymers.* 15: 219–225.

Kachalova, G. S., V. M. Morozov, T. Ya. Morozova, E. T. Myachin, A. A. Vagin, B. V. Strokopytov, and Yu. V. Nekrasov. 1991. Comparison of structures of dry and wet hen egg-white lysozyme molecule at 1.8 Å resolution. *FEBS Lett.* 284:91–94.

Kuntz, I. D., and W. Kauzmann. 1974. Hydration of proteins and polypeptides. *Adv. Protein Chem.* 28:239–345.

Kurinov, I. V., and R. W. Harrison. 1995. The influence of temperature on lysozyme crystals. Structure and dynamics of protein and water. *Acta Crystallogr.* D51:98–109.

Lindsay, S. M., S. A. Lee, J. W. Powell, T. Weidlich, C. Demarco, G. D. Lewen, N. J. Tao, and A. Rupprecht. 1988. The origin of the A to B transition in DNA fibers and films. *Biopolymers.* 27:1015–1043.

Mizoguchi, K., Y. Hori, and Y. Tominaga. 1992. Study on dynamical structure in water and heavy water by low-frequency Raman spectroscopy. *J. Chem. Phys.* 97:1961–1968.

Morozov, V. N., T. Ya. Morozova, G. S. Kachalova, and E. T. Myachin. 1988. Interpretation of water desorption isotherms of lysozyme. *Int. J. Biol. Macromol.* 10:329–336.

Mrevlishvili, G. M. 1984. Low-temperature Calorimetry on Biological Macromolecules. Metsniereba, Tbilisi, Georgia.

Otting, G., and K. Wunthrich. 1989. Studies of protein hydration in aqueous solution by direct NMR observation of individual protein-bound water molecules. *J. Am. Chem. Soc.* 111:1871–1875.

Pethig, R. 1992. Protein-water interactions determined by dielectric methods. *Annu. Rev. Phys. Chem.* 43:177–205.

Rupprecht, A. 1966. Preparation of oriented DNA by wet spinning. *Acta Chem. Scand.* 20:494–504.

Rupprecht, A., and B. Forslind. 1970. Variation of electrolyte content in wet-spun lithium- and sodium-DNA. *Biochim. Biophys. Acta.* 204: 304–316.

Shuker, R., and R. W. Gammon. 1970. Raman-scattering selection-rule breaking and the density of states in amorphous materials. *Phys. Rev. Lett.* 25:222–225.

Steinrauf, L. K. 1959. Preliminary X-ray data for some new crystalline forms of β-lactoglobulin and hen egg-white lysozyme. *Acta Crystallogr.* 12:77–78.

Sugawara, Y., N. Kamiya, H. Iwasaki, T. Ito, and Y. Satow. 1991. Humidity-controlled reversible structure transition of disodium adenosine 5′-triphosphate between dihydrate and trihydrate in a single crystal state. *J. Am. Chem. Soc.* 113:5440–5445.

Tao, N. J., S. M. Lindsay, and A. Rupprecht. 1987. The dynamics of the DNA hydration shell at gigahertz frequencies. *Biopolymers.* 26: 171–188.

Tominaga, Y., M. Shida, K. Kubota, H. Urabe, Y. Nishimura, and M.

Tsuboi. 1985. Coupled dynamics between DNA double helix and hydrated water by low-frequency Raman spectroscopy. *J. Chem. Phys.* 83:5972–5975.

Urabe, H., Y. Sugawara, M. Tsukakoshi, and T. Kasuya. 1991. Low-frequency Raman spectra of guanosine and nucleotides in ordered states: origin of the lowest-frequency mode. *J. Chem. Phys.* 95:5519–5523.

Urabe, H., and Y. Tominaga. 1982. Low-lying collective modes of DNA double helix by Raman spectroscopy. *Biopolymers.* 21:2477–2481.

Weidlich, T. 1989. Raman spectroscopy from the low frequency vibrations of DNA in highly crystalline film, oligonucleotide crystals and polynucleotide solutions. Ph.D. dissertation. Arizona State University, Tempe.

Weidlich, T., S. M. Lindsay, Qi Rui, A. Rupprecht, W. L. Peticolas, and G. A. Thomas. 1990. A Raman study of low frequency interahelical modes in A-, B-, and C-DNA. *J. Biomol. Struct. Dyn.* 8:139–171.

Young, A. C. M., J. C. Dewan, C. Nave, and R. F. Tilton. 1993. Comparison of radiation-induced decay and structure refinement from x-ray data collected from lysozyme crystals at low and ambient temperatures. *J. Appl. Crystallogr.* 26:309–319.